Journal of Organometallic Chemistry 655 (2002) 146–157

Journal of Organo metallic Chemistry

www.elsevier.com/locate/jorganchem

Iron(II) complexes containing poly(1-pyrazolyl)methane ligands

Leslie D. Field [a],*, Barbara A. Messerle [b],*, Linnea P. Soler [a], Trevor W. Hambley [a], Peter Turner [a]

[a] School of Chemistry, University of Sydney, Sydney, NSW 2006, Australia
[b] School of Chemistry, University of New South Wales, Sydney, NSW 2052, Australia

Received 23 November 2001; accepted 8 April 2002

Abstract

A number of iron(II) compounds containing the poly(1-pyrazolyl)methane ligands bis(1-pyrazoyl)methane (BPM, **3**), bis(3,5-dimethyl-1-pyrazolyl)methane (dmBPM, **4**), and *tris*(1-pyrazolyl)methane (TPM, **2**), were synthesised and characterised: *cis*-[$Fe(BPM)_2Cl_2$] (**5**), *trans*-[$Fe(BPM)_2(NCS)_2$] (**9**), [$Fe(BPM)_2Cl]^+(BPh_4)^-$ (**7**), [$Fe(dmBPM)_2Cl_2$] (**6**), [$Fe(dmBPM)_2Cl]^+(BPh_4)^-$ (**8**), [$Fe(TPM)_2]^{2+}(Cl^-)_2$ (**10**), and [$Fe(TPM)(NCS)_2$] (**11**). The solid-state structures of *cis*-[$Fe(BPM)_2Cl_2$] (**5**) and *trans*-[$Fe(BPM)_2(NCS)_2$] (**9**) were determined by single crystal X-ray diffraction analysis. The compound *cis*-[$Fe(BPM)_2Cl_2$] (**5**) crystallises as colourless prisms from ethanol and *trans*-[$Fe(BPM)_2(NCS)_2$] (**9**) crystallises as colourless plates from methanol. All complexes were characterised by ^{1}H- and ^{13}C-NMR spectroscopy, infrared and far infrared spectroscopy, and mass spectroscopy. All of the iron(II) poly(1-pyrazolyl)methane compounds display temperature-dependent paramagnetism. © 2002 Elsevier Science B.V. All rights reserved.

Keywords: Transition metals; Pyrazolylmethane; N ligands; Iron; Temperature dependent paramagnetism

1. Introduction

Iron complexes containing N-donor ligands can be active as homogeneous catalysts for the conversion of simple hydrocarbons. For example, iron complexes containing the bidentate nitrogen-donor ligand, 1,4-diaza-1,3-diene (DAD), act as precursors for selective and substrate specific catalytic reactions including [4+2] cycloadditions of simple dienes [1] and the cyclodimerisation of 1,3-dienes [2]. Metalloenzymes containing iron centres catalyse a range of processes, including oxygen transport and the reduction of N_2 [3]. N-donor ligands have been widely used in model compounds to mimic the metal N-donor imidazolyl side-chains of histidine in proteins [3].

Trofimenko initiated the investigation into the use of poly(1-pyrazolyl)borates (PPB) to model histidine donors and this has led to the synthesis of a range of poly(1-pyrazolyl)borate iron complexes, several of which act as biomimetic compounds [4]. *tris*(1-Pyrazolyl)borate (TPB, **1**) has been used to structurally mimic the three histidine residues in the preparation of a hemerythrin analogue [5], as well as model methane monooxygenase [6]. Several neutral octahedral complexes have been reported where two tridentate (1-pyrazolyl)borate ligands are bound to an iron(II) centre such as [$Fe(TPB)_2$], and [$Fe(dmTPB)_2$] (*tris*(3,5-dimethyl-1-pyrazolyl)borate dmTPB), and these complexes commonly exhibit spin state transition behaviour [7,8]. Iron(II) complexes containing only one tridentate PPB ligand bound to the metal centre have also been reported, e.g. [$Fe(TPB)(CO)_2(C_3F_7)$] [9], and also complexes with optically active PPB ligands [10]. There are fewer examples of iron(II) complexes containing bidentate pyrazolylborate ligands [7,9].

Although the neutral poly(1-pyrazoyl)alkane (PPA) ligands are isosteric with the poly(1-pyrazolyl)borate (PPB) ligands, few iron PPM complexes have been reported. *tris*(1-Pyrazolyl)methane (TPM, **2**) iron complexes synthesised to date include a neutral monomeric iron(III) complex [$Fe(TPM)Cl_3$] [11] and the cationic monomeric iron(II) complexes [$Fe(TPM)_2]^{2+}(X^-)_2$ ($X = ClO_4^-$) [12] ($X = Br^-$) [13]. The neutral complex

---

* Corresponding authors. Fax: +61-2-9351-6650.
E-mail address: l.field@chem.usyd.edu.au (L.D. Field).

PII: S0022-328X(02)01471-7

$[Fe(TPM)(NCS)_2]_n$ [13] is reported to be six-coordinate and is thought to be polymeric with thiocyanate bridging the iron centres. TPM behaves as a bidentate ligand in the six-coordinate octahedral iron complex *trans*-$[Fe(\kappa^2\text{-TPM})(PMe_3)_2(CO)(COMe)]^+(BPh_4)^-$ [14]. The $[Fe(TPM)_2]^{2+}$ cation has been characterised crystallographically [15] and undergoes a low-spin to high-spin crossover near 270 K. Similarly, iron(II) complexes with the *tris*(3,5-dimethyl-1-pyrazolyl)methane ligand have been observed to exhibit low-spin to high-spin crossover [16].

One iron compound containing the bis(1-pyrazoyl)methane (BPM, **3**) ligand has been reported-*trans*-$[Fe(BPM)(PMe_3)_2(CO)(COMe)]^+(BPh_4)^-$ [14]. The bis(3,5-dimethyl-1-pyrazolyl)methane (dmBPM, **4**) ligand has also been used in the synthesis of iron(II) complexes, including the synthesis of neutral complexes which contain just one bidentate ligand, e.g. $[Fe(dmBPM)X_2]$ ($X = Cl^-$, Br^-), or two bidentate ligands, e.g. *trans*-$[Fe(dmBPM)_2(NCS)_2]$ [13]. All cationic complexes reported have two dmBPM (**4**) ligands per iron centre and the majority of these complexes are five-coordinate, e.g. $[Fe(dmBPM)_2(X)]^+Y^-$ ($X = Cl$, $Y = (BPh_4)^-$) ($X = Br$, $Y = (BPh_4)^-$) ($X = I$, $Y = I^-$) [13].

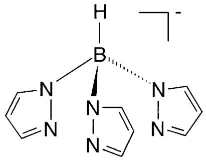
(1)

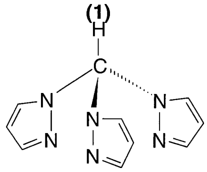
(2)

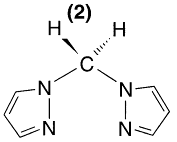
(3)

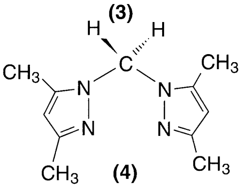
(4)

Poly(1-pyrazolyl)alkane ligands (PPA) afford several advantages in the synthesis of iron complexes containing N-donor ligands. PPA ligands are neutral, and as such are appropriate mimics of the naturally occurring histidine residues found in metalloenzymes. In addition, the boron-bound hydrides of the PPB ligand are known to be reactive and there have been reports of interaction of the B–H residue with the metal centre [17].

In this paper, we report the synthesis and characterisation of a number of iron(II) compounds containing the poly(1-pyrazolyl)methane ligands BPM (**3**), dmBPM (**4**), and TPM (**2**): *cis*-$[Fe(BPM)_2Cl_2]$ (**5**), $[Fe(dmBPM)_2Cl_2]$ (**6**), $[Fe(BPM)_2Cl]^+(BPh_4)^-$ (**7**), $[Fe(dmBPM)_2Cl]^+(BPh_4)^-$ (**8**) [13], *trans*-$[Fe(BPM)_2(NCS)_2]$ (**9**) $[Fe(TPM)_2]^{2+}(Cl^-)_2$ (**10**), and $[Fe(TPM)(NCS)_2]$ (**11**). The solid-state structures of *cis*-$[Fe(BPM)_2Cl_2]$ (**5**) and *trans*-$[Fe(BPM)_2(NCS)_2]$ (**9**) were determined by single crystal X-ray diffraction analysis.

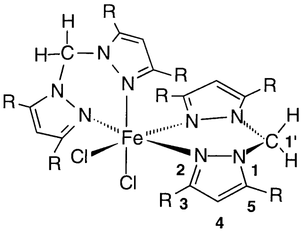
5 R = H
6 R = CH_3

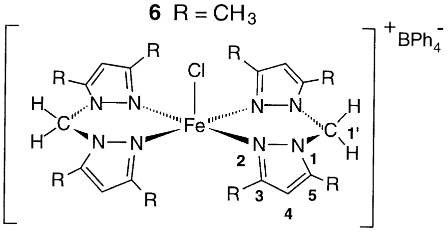
7 R = H
8 R = CH_3

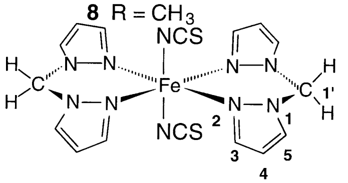
9

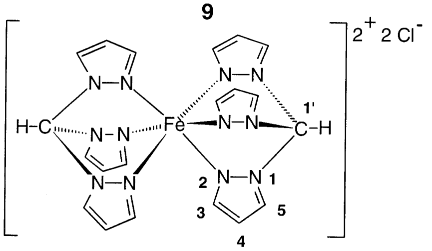
10

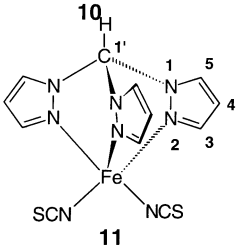
11

2. Discussion

2.1. Synthesis of bis(1-pyrazolyl)methane (BPM) iron(II) complexes

2.1.1. Synthesis of *cis*-[Fe(BPM)$_2$Cl$_2$] (5) and *trans*-[Fe(BPM)$_2$(NCS)$_2$] (9)

Both *cis*-[Fe(BPM)$_2$Cl$_2$] (**5**) and *trans*-[Fe(BPM)$_2$(NCS)$_2$] (**9**) were synthesised by the reaction of one equivalent of the appropriate iron(II) precursor with ca. two equivalents of the BPM ligand (**3**). Reaction of the precursor [FeCl$_2$] in ethanol with BPM afforded *cis*-[Fe(BPM)$_2$Cl$_2$] (**5**) as a white crystalline air-stable powder in 89% yield. Reaction of BPM with the precursor [Fe(NCS)$_2$] in methanol resulted in the formation of *trans*-[Fe(BPM)$_2$(NCS)$_2$] (**9**) as white air-stable crystals in 87% yield.

Both *cis*-[Fe(BPM)$_2$Cl$_2$] (**5**) and *trans*-[Fe(BPM)$_2$(NCS)$_2$] (**9**) are neutral, six-coordinate, octahedral complexes with two BPM ligands bound to an iron(II) centre. In complex (**5**) the two bidentate BPM ligands are bound in a fashion such that the two chloro ligands are mutually *cis*, whereas the two bidentate BPM ligands in complex (**9**) are bound *trans* to each other such that the two isothiocyanate ligands are mutually *trans*.

2.1.2. X-ray crystal structures of *cis*-[Fe(BPM)$_2$Cl$_2$] (5) and *trans*-[Fe(BPM)$_2$(NCS)$_2$] (9)

The solid-state structures of *cis*-[Fe(BPM)$_2$Cl$_2$] (**5**) and *trans*-[Fe(BPM)$_2$(NCS)$_2$] (**9**) were determined by single crystal X-ray diffraction analysis. Crystal data and structure refinement parameters are given in Table 1. The compound *cis*-[Fe(BPM)$_2$Cl$_2$] (**5**) crystallises as colourless prisms from ethanol. An ORTEP depiction of (**5**), including the atom numbering scheme, is shown in Fig. 1. The complex *trans*-[Fe(BPM)$_2$(NCS)$_2$] (**9**) crystallises as colourless plates from methanol. An ORTEP depiction of (**9**), including the atom numbering scheme, is shown in Fig. 2. The bond angles and bond lengths for the inner coordination sphere of (**5**) and (**9**) are listed in Tables 2 and 3, respectively.

The complexes *cis*-[Fe(BPM)$_2$Cl$_2$] (**5**) and *trans*-[Fe(BPM)$_2$(NCS)$_2$] (**9**) are essentially octahedral about the iron centre. Some distortion arises from the two coordinating nitrogen atoms of the pyrazolyl rings from each ligand being constrained to a tighter bite angle by the architecture of the ligand. The N–Fe–N angle is further compressed in the *cis* complex (**5**) by the two bulky *cis*-chloro ligands and by the steric requirements of interleaving the pyrazolyl rings belonging to the two ligands which are forced to interact due to their proximity. The two BPM ligands in the *trans*-complex (**9**) are, however relatively unhindered and the N–Fe–N angle of each BPM ligand is larger than those observed in the *cis* complex (**5**) (Table 2).

Table 1

Crystal data and structure refinement parameters for *cis*-[Fe(BPM)2Cl2] (**5**) and *trans*-[Fe(BPM)2(NCS)2] (**9**)

	cis-[Fe(BPM)$_2$Cl$_2$] (**5**)	*trans*-[Fe(BPM)$_2$(NCS)$_2$] (**9**)
Empirical formula	$C_{14}H_{16}N_8Cl_2Fe$	$C_{16}H_{16}FeN_{10}S_2$
Formula weight	423.09	468.34
Crystal colour, habit	Colourless, prism	Colourless, plate
Crystal dimensions (mm)	0.17 × 0.17 × 0.17	0.22 × 0.22 × 0.01
A (Å)	7.4482(8)	8.1135(9)
B (Å)	13.214(2)	15.7862(8)
C (Å)	18.315(2)	8.730(1)
β (°)	94.529(8)	114.03(1)
V (Å^3)	1796.9(3)	1021.2(2)
Crystal system	Monoclinic	Monoclinic
Space group	$P2_1/n$ (#14)	$P2_1/a$ (#14)
Z value	4	2
D_{calc} (g cm^{-3})	1.564	1.523
F(000)	864.00	480.00
μ(Mo–K$_\alpha$) (mm^{-1})	1.1520	8.053
Radiation	Mo–K$_\alpha$ ($\lambda = 0.71069$ Å)	Cu–K$_\alpha$ ($\lambda = 1.54178$ Å)
$2\theta_{max}$ (°)	49.9	120.1
hkl Range	−8 8, −1 15, −1 21	0 9, 0 17, −9 8
Number of reflections measured	Total: 3948, unique: 3144 ($R_{int} = 0.015$)	Total: 1709, unique: ($R_{int} = 0.044$)
Number of observations ($I > 2.00\sigma(I)$)	2730	998
Number of variables	226	133
Transmission factors	Analytical: 0.824, 0.853	Empirical: 0.42–0.99
Residuals [a]: R_1; wR_2 (all data)	0.0274; 0.0675	0.0409; 0.1173
Weighting scheme, where $P = (F_o^2 + 2F_c^2)/3$	$1/[\sigma^2(F_o^2) + (0.0285P)^2 + 0.6710P]$	$1/[\sigma^2(F_o^2) + (0.05P)^2]$
Goodness-of-fit (all data)	1.028	1.248
Residual extrema (e Å^{-3})	−0.229, 0.167	−0.244, 0.557

[a] $R_1 = \Sigma||F_o| - |F_c||/\Sigma|F_o|$ for $F_o > 2\sigma(F_o)$; $wR_2 = (\Sigma w(F_o^2 - F_c^2)^2/\Sigma(wF_c^2)^2)^{1/2}$ all reflections; w is defined in the table.

The complex *trans*-[Fe(BPM)$_2$(NCS)$_2$] (**9**) has an inversion centre and accordingly all three *trans* bond angles through the iron centre of (**9**) are 180° and the iron centre is contained within the three coordination planes. The complex *cis*-[Fe(BPM)$_2$Cl$_2$] (**5**) deviates slightly from perfect octahedral coordination, with the dihedral angles between the least squares planes which define the octahedral coordination of (**5**) being 90.74(4), 91.57(4), and 91.21(4)° and with the deviation from these least squares planes being only 0.017(6), 0.058(5), and 0.018(5) Å. The pyrazolyl rings of both (**5**) and (**9**) are essentially planar.

There is nearly perfect tetrahedral symmetry about the bridgehead carbon atom of the BPM ligands in the *trans*-complex (**9**), while some compression occurs at the bridgehead atoms in the *cis*-complex (**5**). The distortion in (**5**) is most likely due to the ligand being folded into a

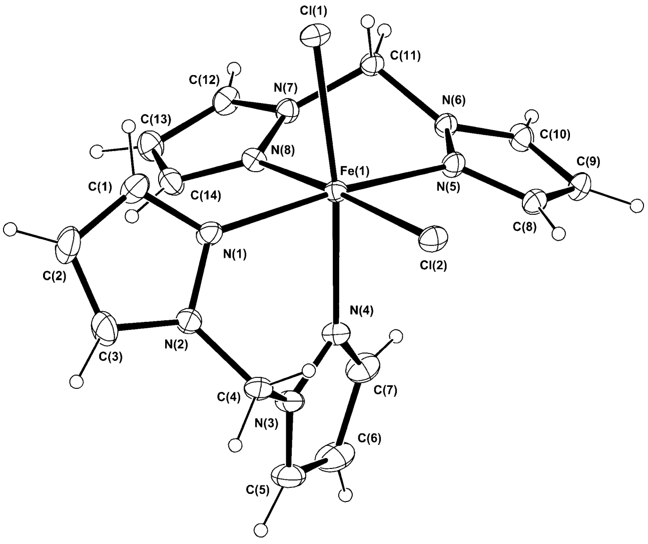

Fig. 1. ORTEP depiction, with atom numbering and 20% displacement ellipsoids, of *cis*-[Fe(BPM)$_2$Cl$_2$] (**5**).

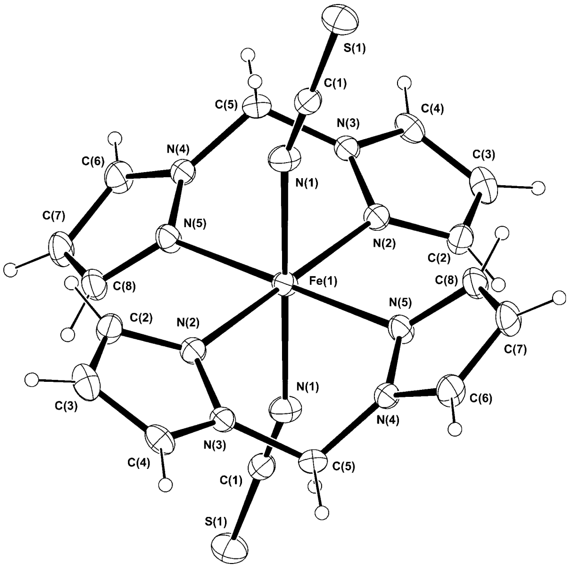

Fig. 2. ORTEP depictions, with 20% displacement ellipsoids, of *trans*-[Fe(BPM)$_2$(NCS)$_2$] (**9**). The complex resides on an inversion site and the equivalent atoms are generated with $1-x$, $-y$, $-z$.

Table 2
Selected bond angles for *cis*-[Fe(BPM)$_2$Cl$_2$] (**5**) and *trans*-[Fe(BPM)$_2$(NCS)$_2$] (**9**)

cis-[Fe(BPM)$_2$Cl$_2$] (**5**)		*trans*-[Fe(BPM)$_2$(NCS)$_2$] (**9**)	
Atoms	Bond angles (°)	Atoms	Bond angles (°)
Cl(1)–Fe–Cl(2)	98.32(2)	N(1)–Fe–N(1^a)	180
Cl(1)–Fe–N(5)	94.82(5)	N(2)–Fe–N(2^a)	180
Cl(1)–Fe–N(8)	87.48(5)	N(5)–Fe–N(5^a)	180
Cl(1)–Fe–N(1)	92.72(5)	N(1)–Fe–N(2)	90.42(13)
Cl(1)–Fe–N(4)	171.06(5)	N(1)–Fe–N(5)	86.65(13)
Cl(2)–Fe–N(5)	91.31(5)	N(2)–Fe–N(5)	86.70(12)
Cl(2)–Fe–N(8)	173.48(5)		
Cl(2)–Fe–N(1)	95.07(5)		
Cl(2)–Fe–N(4)	90.17(5)		
N(1)–Fe–N(4)	83.68(7)		
N(5)–Fe–N(8)	85.19(7)		
N(1)–Fe–N(5)	169.33(7)		

[a] Related by inversion operation $1-x$, $-y$, $-z$.

Table 3
Selected bond lengths for *cis*-[Fe(BPM)$_2$Cl$_2$] (**5**) and *trans*-[Fe(BPM)$_2$(NCS)$_2$] (**9**)

cis-[Fe(BPM)$_2$Cl$_2$] (**5**)		*trans*-[Fe(BPM)$_2$(NCS)$_2$] (**9**)	
Atoms	Bond distances (Å)	Atoms	Bond distances (Å)
Fe–Cl(1)	2.4245(6)	Fe–N(1)	2.140(4)
Fe–Cl(2)	2.4590(7)	Fe–N(2)	2.198(3)
Fe–N(1)	2.1997(18)	Fe–N(5)	2.197(3)
Fe–N(4)	2.2569(18)	–	–
Fe–N(5)	2.1863(18)	–	–
Fe–N(8)	2.2635(18)	–	–

boat conformation. Because the two BPM ligands are bound *trans* to each other in (**9**), steric interference is minimised to an extent that the boat conformation of the [Fe(NN)$_2$C] metallacycle is very shallow and less distortion occurs about the bridgehead carbon.

The Fe–N(BPM) bond lengths of BPM which are *trans* to an N atom are similar for both *cis*-[Fe(BPM)$_2$Cl$_2$] (**5**) and *trans*-[Fe(BPM)$_2$(NCS)$_2$] (**9**) and lie in the range of 2.1863(18)–2.198(3) Å (Table 3). The Fe–N(BPM) bonds *trans* to a chloride atom in (**5**) are, at 2.2569(18) and 2.2635(18) Å, longer than those *trans* to a nitrogen atom. The Fe–Cl bonds in (**5**), 2.4245(6) and 2.4590(7) Å, are likewise longer than the Fe–N(BPM) bonds within the same complex. The Fe–N(NCS) bonds of the isothiocyanato ligands in complex (**9**), 2.140(4) Å, are shorter than the Fe–N(BPM) bonds of the ligand.

Although the oxidation state of the metal centre is different, the structure of (**5**) is similar to that of several *cis*-dichloro iron(III) complexes, [Fe(NN)$_2$Cl$_2$]$^+$, which also have two bidentate N-donor ligands bound to the iron centre {(NN = bipy, **12**) [18], (NN = 2,2′-biimidazole(biimm), **13**) [19], (NN = phen, **14**) [20]}. Several iron complexes have been reported in which two isothiocyanate ligands are bound to an iron centre, e.g. *cis*-[Fe(bipy)$_2$(NCS)$_2$] [21,22]. However, no iron complexes that contain two bidentate N-donor ligands have yet been reported where the other two co-ligands, such as Cl or NCS, are bound mutually *trans*. The basic structural elements of the two iron(II) PPM complexes, *cis*-[Fe(BPM)$_2$Cl$_2$] (**5**) and *trans*-[Fe(BPM)$_2$(NCS)$_2$] (**9**), the three iron(III) complexes containing two bidentate N-donor ligands, [Fe(NN)$_2$Cl$_2$]$^+$ (**12**, **13**, and **14**), and the ruthenium(II) PPM structures, [(PPh$_3$)(BPM)Ru-(μ-Cl)$_3$-Ru(PPh$_3$)(BPM)]$^+$Cl$^-$ (**15**) and [RuCl(PPh$_3$)$_2$-(TPM)]$^+$Cl$^-$ (**16**; Cl$^-$), are given in Tables 4 and 5 for comparison.

The N–M–N bond angle within the bidentate BPM ligand is similar in both the iron(II) and the ruthenium(II) complexes (Table 4). The N–M–N bond angle of the bidentate BPM ligands is larger than the N–M–N angle for bipy, phen, and biimm ligands, due to the structural constraints of the individual ligands. The *cis*-(Cl–M–Cl) angle is similar for the iron(II) complex and the iron(III) complexes. The *cis*-(Cl–M–Cl) bond angle is larger than the *cis*-(SCN–Fe–NCS) bond angle which may be due to the larger steric bulk of the chloro ligands.

A comparison of bond lengths (Table 5) shows that the M–Cl bonds *trans* to the N donor atom of either BPM or TPM are similar (2.396–2.459 Å). The bond distance range for the iron(III) complexes is 2.326–2.252 Å. Fe–N bonds *trans* to a chlorine atom are consistently longer than Fe–N bonds *trans* to a nitrogen atom. Inspection of the Fe–N bond lengths of the bound N-donor ligand reveals the trend that the Fe–N *trans* to a N-donor atom are consistently shorter than those *trans* to a Cl-ligand. The M–N bonds are longer in the iron(II) PPM complexes than in the ruthenium(II) PPM complexes. The Fe–N bonds of the ligands of both BPM complexes are similar.

2.1.3. Mass spectra of *cis*-[$Fe(BPM)_2Cl_2$] (5)

The complex *cis*-[$Fe(BPM)_2Cl_2$] (**5**), was examined by CI mass spectroscopy (NH_3 and CH_4 ionisation) and electrospray ionisation (with methanol as the carrier solvent). All mass spectra contained peaks consistent with the molecular weight of the parent ion (422 AMU) as well as a peak (387 AMU) which is consistent with the cation, [$Fe(BPM)_2Cl]^+$. Both of these peaks display isotope distribution patterns that are consistent with those simulated for a monomeric complex.

2.1.4. Infra-red spectra of *cis*-[$Fe(BPM)_2Cl_2$] (5) and *trans*-[$Fe(BPM)_2(NCS)_2$] (9)

Confirmation of the presence of metal-bound chloro ligands was obtained by far infrared spectroscopy. The far infrared spectrum of *cis*-[$Fe(BPM)_2Cl_2$] (**5**) contains two bands at 390 and 350 cm^{-1} (by diffuse reflectance spectroscopy in a polyetheylene matrix), suggesting that the iron complex has two iron-bound chloro ligands which are mutually *cis* [23,24]. A distinct band in the far infrared region (278 cm^{-1}) was assigned to an iron–nitrogen stretch.

The NCS ligand can bind to the metal centre through its nitrogen atom, i.e. as an isothiocyanato ligand, or through its sulphur atom, i.e. as a thiocyanato ligand. The infrared spectrum of *trans*-[$Fe(BPM)_2(NCS)_2$] (**9**) was acquired using a powdered KBr matrix and diffuse reflectance spectroscopy. The spectrum, with δ(NCS) at 480 cm^{-1}, ν(CS) at 769 cm^{-1}, and ν(CN) at 2075 and 2064 cm^{-1}, indicates that [$Fe(BPM)_2(NCS)_2$] (**9**), in the solid-state, has two *trans*-bound isothiocyanato ligands [23,24].

Table 4
Selected bond angles (°) of *cis*-[$Fe(BPM)_2Cl_2$] (**5**), *trans*-[$Fe(BPM)_2(NCS)_2$] (**9**), [$Fe(bipy)_2Cl_2]^+$ (**12**) (bipy = bipyridine) [18], [$Fe(biimm)_2Cl_2]^+$ (**13**) (biimm = 2,2′-biimidazole) [19], [$Fe(phen)_2Cl_2]^+$ (**14**) (phen = 1,10-phenanthroline) [20], [(PPh_3)-(BPM)Ru-(μ-Cl)$_3$-Ru(PPh_3)(BPM)]$^+Cl^-$ (**15**), and [$RuCl(PPh_3)_2$-(TPM)]$^+Cl^-$ (**16**; Cl^-)

Atoms	Bond angles (°)						
	Fe(II)		Fe(III)			Ru(II)	
Complex	**5**	**9**	**12**	**13**	**14**	**15**	**16**
Cl–M–Cl	98.32	–	101.6	95.11	99.81	–	–
N–M–N [a]	83.68	86.7	74.9	76.91	76.30	87.7	–
N–M–N [a]	85.19	86.7	75.6	76.37	76.30	88.4	–

[a] N–M–N angle as defined by the metallocycle formed from one bidentate ligand binding to the metal centre.

2.1.5. ^1H-NMR spectra of *cis*-[$Fe(BPM)_2Cl_2$] (5) and *trans*-[$Fe(BPM)_2(NCS)_2$] (9)

At 300K (or at higher temperatures) no signals due to the bound BPM (**3**) ligands of the *cis*-[$Fe(BPM)_2Cl_2$] (**5**) complex were present in the ^1H-NMR spectrum. However, by reducing the temperature of the sample, four peaks of equivalent intensity developed in the ^1H-NMR spectrum (Fig. 3). The sharpest spectrum was observed at 234 K, however the resonances were still broadened and no interproton couplings were observed (Fig. 3). At temperatures below 234 K, the resonances again broadened with decreasing temperature. This behaviour is consistent with temperature-dependent paramagnetism which has been observed previously in Fe(II) complexes containing pyrazolyl ligands [25,15,16]. The four resonances observed, due to the three backbone protons of a pyrazolyl ring (**H**3, **H**4, and **H**5) and the geminal protons (**H**1′) of the BPM ligand, indicate that, in solution, the complex has C_{2V} symmetry (or at least dynamic C_{2V} symmetry). The equivalence of the pyrazolyl rings indicates a rapid *cis*–*cis* exchange process occurs or that, in solution, the complex adopts a *trans* geometry.

Although proton resonances are visible in the ^1H-NMR spectrum of [$Fe(BPM)_2(NCS)_2$] (**9**) acquired at 300 K, lowering the acquisition temperature to 250K resulted in sharper resonances and two of the BPM resonances were resolved. This is consistent with a *trans*-geometry for (**9**).

2.1.6. Synthesis and characterisation of [$Fe(BPM)_2Cl]^+(BPh_4)^-$ (7)

The cationic iron(II) complex [$Fe(BPM)_2$-Cl]$^+(BPh_4)^-$ (**7**) was synthesised from [$FeCl_2$], BPM

Table 5
Selected bond lengths (Å) of *cis*-$[Fe(BPM)_2Cl_2]$ (**5**), *trans*-$[Fe(BPM)_2(NCS)_2]$ (**9**), $[Fe(bipy)_2Cl_2]^+$ (**12**) (bipy = bipyridine) [18], $[Fe(biimm)_2Cl_2]^+$ (**13**) (biimm = 2,2′-biimidazole) [19], $[Fe(phen)_2Cl_2]^+$ (**14**) (phen = 1,10-phenanthroline) [20], $[(PPh_3)(BPM)Ru\text{-}(\mu\text{-}Cl)_3\text{-}Ru(PPh_3)(BPM)]^+Cl^-$ (**15**), and $[RuCl(PPh_3)_2(TPM)]^+Cl^-$ (**16**; Cl^-)

Atoms	Bond distances (Å)						
	Fe(II)		Fe(III)			Ru(II)	
Complex	**5**	**9**	**12**	**13**	**14**	**15**	**16**
M–Cl [a]	2.4245	–	2.252	2.290	2.252	2.422	2.402
M–Cl [a]	2.4590	–	2.258	2.326	2.243	2.396	–
M–N [b]	2.1997	2.197	2.120	2.108	2.16	–	2.117 [d]
M–N [b]	2.1863	2.198	2.122	2.112	2.14	–	2.126 [d]
M–N [c]	2.2569	–	2.198	2.152	2.19	–	2.083
M–N [c]	2.2635	–	2.188	2.209	2.23	–	–

[a] M–Cl bond *trans* to N.
[b] M–N bond *trans* to N.
[c] M–N bond *trans* to Cl.
[d] M–N bond *trans* to P.

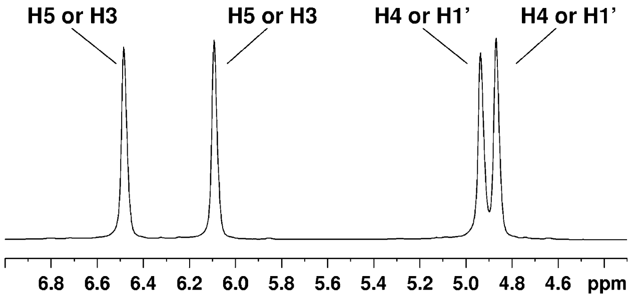

Fig. 3. ^1H-NMR (400 MHz) spectrum of *cis*-$[Fe(BPM)_2Cl_2]$ (**5**) in d^4-MeOH at 234 K.

(**3**), and $NaBPh_4$ in hot ethanol and was isolated as a white powder in 85% yield. $[Fe(BPM)_2Cl]^+(BPh_4)^-$ (**7**) is a uni-positive cationic five-coordinate complex which contains one tetraphenylborate anion, $(BPh_4)^-$, per iron(II) cation. Integration of the ^1H-NMR spectrum indicated a ratio of two BPM ligands per $(BPh_4)^-$ counterion. The molecular weight (449 AMU) of the parent ion observed in the mass spectrum of $[Fe(BPM)_2Cl]^+(BPh_4)^-$ (**7**) was consistent with a monomeric uni-positive iron complex that contains two BPM ligands and one chloro ligand. The presence of an Fe–Cl bond in (**7**) was also confirmed by far infrared spectroscopy, (by diffuse reflectance recorded in a polyethylene matrix). A band attributed to an Fe–Cl stretch was observed at 408 cm^{-1} and a band due to the Fe–N stretch was observed in the far infrared region at 277 cm^{-1}.

Only the proton resonances of the $(BPh_4)^-$ anion were visible in the ^1H-NMR spectrum of $[Fe(BPM)_2Cl]^+(BPh_4)^-$ (**7**) acquired at 300 K. As the temperature was reduced, resonances of the BPM protons became visible and the signals continued to sharpen as the temperature was lowered. The sharpest ^1H-NMR spectrum was acquired at 233 K and four signals (**H**3, **H**4, **H**5, and **H**1′) from two symmetrically bound BPM ligands were observed in addition to the signals from the $(BPh_4)^-$ anion. Below this temperature, the peaks due to the anion broadened significantly. A ^{13}C-NMR spectrum was acquired at 240 K and verified the presence of BPM and $(BPh_4)^-$ in the iron complex.

2.2. Synthesis of bis(3,5-dimethyl-1-pyrazolyl)methane (dmBPM) iron(II) complexes

2.2.1. Synthesis and characterisation of $[Fe(dmBPM)_2Cl_2]$ (*6*)

The reaction of $[FeCl_2]$ with dmBPM (**4**), in a 1:2 molar ratio, produced the neutral complex, $[Fe(dmBPM)_2Cl_2]$ (**6**), as a white powder in excellent yield. The molecular weight of the parent ion in the mass spectrum is consistent with an iron complex containing two dmBPM ligands and two chloro ligands. The far infrared spectrum contains two bands at 350 and 322 cm^{-1} that suggests that the two chloro ligands are mutually *cis* in the solid-state. Confirmation that the dmBPM ligands are bound to the metal centre is also found in the far infrared spectrum with an Fe–N stretch at 278 cm^{-1}.

At 300 K only very broad signals are observed in the baseline of the ^1H-NMR spectrum of $[Fe(dmBPM)_2Cl_2]$ (**6**). However, on decreasing the temperature to 228 K, four proton resonances, attributed to the C3-$\mathbf{CH_3}$, **H**4, C5-$\mathbf{CH_3}$, and **H**1′ protons of dmBPM, were observed. This suggests that both the pyrazolyl rings and the dmBPM ligands are chemically equivalent. Based on the symmetry of the spectrum, in solution, either the *trans* product predominates, or that there is a rapid exchange between *cis* isomers.

2.2.2. Synthesis and characterisation of $[Fe(dmBPM)_2Cl]^+(BPh_4)^-$ (**8**)

Following the published procedure of Mani [13], $[Fe(dmBPM)_2Cl]^+(BPh_4)^-$ (**8**), was prepared as a white powder, in excellent yield from the reaction between $[FeCl_2]$ and dmBPM (**4**) in the presence of $NaBPh_4$. Mani used magnetic moment measurements, the ligand field spectrum, conductivity tests, and microanalysis to characterise (**8**), and reported that the complex was a five-coordinate uni-positive cationic monomeric complex with a trigonal bipyramidal structure [13].

At 300 K, only the resonances of the $(BPh_4)^-$ anion were observed in the ^{1}H-NMR spectrum of $[Fe(dmBPM)_2Cl]^+(BPh_4^-)$ (**8**), as the signals of the bound ligands were indistinguishable from the baseline. However, in the ^{1}H-NMR spectrum acquired at 228 K, relatively sharp resonances of both the anion and the cation of $[Fe(dmBPM)_2Cl]^+(BPh_4^-)$ (**8**) were observed (Fig. 4). Not only were the pyrazolyl rings and the geminal protons within each dmBPM chemically equivalent in the ^{1}H-NMR spectrum, but the two bound dmBPM ligands were also chemically equivalent. This symmetry led to the observation of only four proton ligand resonances (C3-**CH**$_3$, **H**4, C5-**CH**$_3$, and **H**1′) in the spectrum (Fig. 4). Only six carbon ligand resonances were observed in the $^{13}C\{^1H\}$-NMR spectrum, acquired at 230 K, and were attributed to **C**3, C3-**C**H$_3$, **C**4, **C**5, C5-**C**H$_3$, and **C**1′. Integration of the ^{1}H-NMR spectrum, acquired at 228 K, is consistent with a ratio of two dmBPM ligands per $(BPh_4)^-$ counterion in the iron complex.

The molecular weight of the parent ion, $[Fe(dmBPM)_2Cl]^+$, observed at 499 AMU, is consistent with the proposed formulation and the isotopic distribution pattern in the mass spectrum is consistent with a monomeric uni-positive complex. A band at 353 cm^{-1} in the far infrared spectrum was attributed to the Fe–Cl stretch.

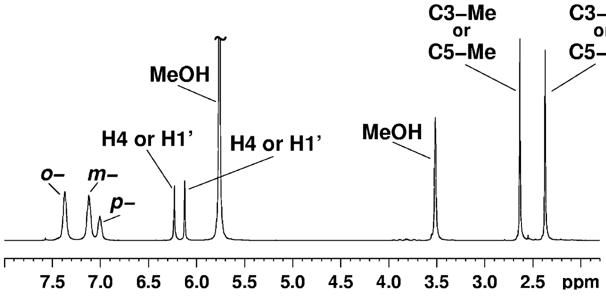

Fig. 4. ^{1}H-NMR spectrum of $[Fe(dmBPM)_2Cl]^+(BPh_4)^-$ (**8**) in d^4-MeOH at 228 K.

2.3. Synthesis of tris(1-pyrazolyl)methane (TPM) iron(II) complexes

2.3.1. Synthesis and characterisation of $[Fe(TPM)_2]^{2+}(Cl^-)_2$ (**10**)

A modification of the synthesis for the previously reported $[Fe(TPM)_2]^{2+}(Br^-)_2$ complex [13] was used for the synthesis of the analogous complex $[Fe(TPM)_2]^{2+}(Cl^-)_2$ (**10**). A colour change from yellow to light purple was observed in the reaction solution upon the addition of the ligand TPM (**2**) to the iron precursor $[FeCl_2]$, and the dipositive iron complex, $[Fe(TPM)_2]^{2+}(Cl^-)_2$ (**10**), was obtained in good yield as a pale purple powder.

The molecular weight of the parent ion (260 AMU) observed in the CI mass spectrum of $[Fe(TPM)_2]^{2+}(Cl^-)_2$ (**10**) was consistent with the dipositive cation, $[Fe(TPM)_2]^{2+}$. The ^{1}H-NMR spectrum of **10** acquired at 300 K contained only two broadened signals for the bound TPM ligands. However, in spectra acquired at lower temperatures, the signals sharpened and shifted so that at 220 K, the spectrum contained three distinct resonances attributed to the backbone protons (**H**3, **H**4, **H**5) on the pyrazolyl ring in addition to a resonance attributed to the geminal proton (**H**1′) of the TPM ligand. Since both TPM ligands are chemically equivalent within the iron complex it is likely that the complex is a symmetric six-coordinate species. The methine proton (**H**1′) resonance of the TPM ligand is labile and exchanges (H/D exchange) with the deuterated methanol solvent after several hours.

2.3.2. Synthesis and characterisation of $[Fe(TPM)(NCS)_2]$ (**11**)

On reaction of $[Fe(NCS)_2]$ with TPM (**2**), a monomeric species $[Fe(TPM)(NCS)_2]$ (**11**), was formed. The product, $[Fe(TPM)(NCS)_2]$ (**11**), was obtained as a light purple solid in a moderate yield. The complex, as a solid, was slightly air-sensitive and, when dissolved, became significantly more air-sensitive. The neutral polymeric complex $[Fe(TPM)(NCS)_2]_n$ was prepared previously by Mani and was reported as a pale green or yellow (almost colourless) six-coordinate, polymeric solid that is inert to aerial oxidation [13].

The parent ion peak in the CI mass spectrum of $[Fe(TPM)(NCS)_2]$ (**11**) indicates that the parent ion consists of one TPM ligand, two NCS ligands, and one iron atom. This suggests that $[Fe(TPM)(NCS)_2]$ (**16**) is five-coordinate. The infrared spectrum of $[Fe(TPM)(NCS)_2]$ (**11**) indicates that the NCS ligands are bound to the iron centre through the nitrogen atoms (2058 cm^{-1}). However, in contrast with reports for the polymeric complex $[Fe(TPM)(NCS)_2]_n$, no bands consistent with a bridging thiocyanate ligand (2105 and 2095 cm^{-1}) were observed in the spectrum of $[Fe(TPM)(NCS)_2]$ (**11**).

At room temperature, the ^{1}H-NMR spectrum of [Fe(TPM)(NCS)$_2$] (**11**) in d^4-MeOH displays broadened resonances which are attributed to the bound TPM ligand. Sharper resonances were observed in the ^{1}H-NMR spectrum acquired at 250 K, which revealed that the three pyrazolyl rings are chemically equivalent. Therefore, at 250 K, the bound TPM ligand of [Fe(TPM)(NCS)$_2$] (**11**) is symmetrical.

3. Experimental

The synthesis and manipulation of all metal complexes was performed under an inert atmosphere of argon or nitrogen using standard Schlenk or vacuum line techniques. All solvents were distilled under a nitrogen atmosphere. Deuterated solvents were first dried, as for their proteo-analogues, then were degassed via three consecutive freeze–pump–thaw cycles, then vacuum distilled and stored under vacuum. All solvents used in air-sensitive reactions were deaerated prior to use either by saturation with nitrogen or via four to five freeze–pump–thaw cycles. All compressed gases were obtained from BOC gases. The following agents were used as received: pyrazole (Aldrich), 3,5-dimethylpyrazole (Aldrich) and sodium tetraphenylborate (Aldrich).

NMR spectra were recorded with a Bruker AMX400 or with a Bruker DRX400 NMR spectrometer at 400.1 (^{1}H), 162.0 (^{31}P), 100.6 (^{13}C) MHz. ^{1}H-NMR and ^{13}C-NMR chemical shifts were referenced internally to residual solvent resonances. Unless otherwise stated, spectra were acquired at 300 K and the temperatures quoted for acquisition of NMR spectra are approximate (± 2 K).

Mass spectra were recorded using electron ionisation (EI), chemical ionisation (CI), fast atom bombardment (FAB), or matrix assisted laser desorption ionisation-time of flight (MALDI-TOF). Data is reported in the form x (y) where x is the mass to charge ratio and y is the percentage abundance relative to the base peak. EI spectra were recorded on an AEI model MS902 double focussing mass spectrometer with an accelerating voltage of 8000 V and using electron impact ionisation with an electron energy of 70 eV. The sample was inserted through a solid direct insertion probe with a source temperature of 200 °C. FAB and CI mass spectra were acquired using a Finnigan MAT TSQ 46 mass spectrometer (San Jose, CA, USA) which was fitted with an electron impact/chemical ionisation (EI/CI) source and a fast atom bombardment (FAB) 8 kV potential gun (ION TECH, Fast Atom Gun, Middlesex, UK). The FABMS were acquired using a 'magic bullet' matrix [a 5:1 (w/w) mixture of dithiothreitol (DTT) (98%) and dithioerythritol (DTE) (98%)] [26], a source temperature of 50 °C, and a manifold temperature of 80 °C. The CI (100 eV electron energy) and EI (70 eV electron energy) mass spectra acquired on the Finnigan MAT TSQ 46 mass spectrometer used a source temperature of 140 °C and a manifold temperature of 115 °C.

Microanalyses were performed by the Chemical Microanalytical Services Pty. Ltd, Melbourne, the Micro Analysis Facility at the University of New South Wales, Sydney, or at the Department of Chemical Engineering at the University of Sydney.

Melting points were determined using either a Reichert heating stage or a Gallenkamp melting point apparatus and are uncorrected.

Infrared spectra (4000–400 cm^{-1}) were recorded using diffuse reflectance techniques on a Bio-Rad FTS-40 spectrometer in DRIFTS mode utilising powdered KBr as the matrix and as the background. Far-infrared spectra (500–250 cm^{-1}) were recorded using diffuse reflectance techniques on a Bio-Rad FTS-40 spectrometer in DRIFTS mode using powdered polyethylene as the matrix and as the background.

3.1. Synthesis of iron precursors

Anhydrous [FeCl$_2$] was prepared following the procedure of Leigh and co-workers [27] and [Fe(NCS)$_2$] was prepared following the procedure developed by Mani [13].

3.2. Synthesis of bis(1-pyrazolyl)methane (BPM) iron(II) complexes

3.2.1. Synthesis of cis-[Fe(BPM)$_2$Cl$_2$] (5)

A solution of [FeCl$_2$] (201 mg, 1.59 mmol) in warm ethanol (5 ml) was added drop-wise to a stirred solution of BPM (**3**) (393 mg, 2.65 mmol) in warm ethanol (5 ml). The clear yellow solution was heated and stirred for 10 min, then allowed to stand undisturbed overnight during which time the product formed as a white precipitate. The white precipitate was isolated by filtration, washed with ethanol (2 × 1 ml) and with hexane (2 × 2 ml), then dried in vacuo to give *cis*-[Fe(BPM)$_2$Cl$_2$] (**5**) as a white crystalline powder (496 mg, 89%).

M.p. decomposes at 218 °C, melts at 221–223 °C. ^{1}H-NMR (400 MHz, d^4-methanol, 234 K): δ 8.15 (brs, 4H, **H**5 or **H**3), 7.76 (brs, 4H, **H**5 or **H**3), 6.61 (brs, 4H, **H**4 or **H**1′), 6.5 (brs, 4H, **H**4 or **H**1′) ppm. (Found: **C**, 39.6; **H**, 3.6; **N**, 26.4. $C_{14}H_{16}N_8Cl_2Fe$ requires **C**, 39.74; **H**, 3.81, **N**, 26.48%.) IR ν_{max} cm^{-1} (polyethylene, diffuse reflectance) 391 (br, *cis*-Fe–Cl), 350 (br, *cis*-Fe–Cl), 277 (s, Fe–N(BPM)). Mass spectrum (CI, NH$_3$, m/z (%)): 424 (11, $M^+ + 2$, $C_{14}H_{18}N_8Cl_2Fe$, [Fe(BPM)$_2$Cl$_2$]+2H), 422 (21, M^+, $C_{14}H_{16}N_8Cl_2Fe$, [Fe(BPM)$_2$Cl$_2$]), 420 (7, $C_{14}H_{14}N_8Cl_2Fe$, [Fe(BPM)$_2$-Cl$_2$]-2H), 389 (46, $C_{14}H_{18}N_8ClFe$, [Fe(BPM)$_2$Cl]$^+$ + 2H), 387 (100, $C_{14}H_{16}N_8ClFe$, [Fe(BPM)$_2$Cl]$^+$), 369

(14), 350 (15), 348 (17), 331 (25), 329 (80), 327 (77), 314 (48).

3.2.2. *cis-[Fe(BPM)$_2$Cl$_2$] (**5**) crystal structure data*

Crystal data together with refinement details are presented in Table 1. A colourless prismatic crystal was inserted in a glass capillary and mounted on an Enraf-Nonius CAD4 diffractometer employing graphite monochromated Mo–K$_\alpha$ radiation. Primitive monoclinic cell constants were obtained from a least-squares refinement using the setting angles of 25 reflections in the range $18.9° < 2\theta < 24.0°$. Data were collected at 295(2) K using $\omega-2\theta$ scans to a maximum 2θ value of 50°. Data reduction and processing was undertaken with the WINGX [28] interface. The intensities of three reference reflections measured every 60 min did not change significantly during the data collection. The crystal faces were indexed and an analytical absorption correction was applied to the data [28,29]. The structure was solved in the space group $P2_1/n$ (#14) by direct methods with SIR92 [30], and extended and refined with SHELXL97 [31] using the TEXSAN [32] interface. Anisotropic displacement parameters were refined for the non-hydrogen of the structure model and a riding atom model was used for the model hydrogen atoms. An ORTEP [33] depiction of the molecule with 20% displacement ellipsoids is provided in Fig. 1.

3.2.3. *Synthesis of trans-[Fe(BPM)$_2$(NCS)$_2$] (**9**)*

A warm magenta solution of [Fe(NCS)$_2$] (159 mg, 0.925 mmol) in methanol (5 ml) was added to a stirred solution of BPM (**3**) (141 mg, 0.952 mmol) in warm methanol (5 ml) to form a clear orange solution. After standing at room temperature (r.t.) for 3 h, the volume was reduced to 5 ml under reduced pressure resulting in the formation of colourless crystals. The product was collected by filtration, washed with methanol (2 × 0.5 ml) and hexane (2 × 1 ml), and dried in vacuo to yield *trans*-[Fe(BPM)$_2$(NCS)$_2$] (**9**) as colourless crystals (433 mg, 90%).

M.p. decomposes at 235 °C, melts at 257–263 °C. ^{1}H-NMR (400 MHz, d^4-methanol, 250 K): δ 8.08 (bs, 4H, **H**5 or **H**3), 7.72 (bs, 4H, **H**5 or **H**3), 6.56 (bs, 4H, **H**4 or **H**1′), 6.50 (bs, 4H, **H**4 or **H**1′) ppm. IR ν_{max} cm^{-1} (KBr powder, diffuse reflectance): 3140 (w), 3114 (w), 3025 (w), 2866 (w), 2075 (vs, CN(NCS)), 2064 (vs, CN(NCS)), 1398 (m), 1286 (m), 1055 (m), 984 (m), 769 (vs, CS(NCS)), 731 (m), 650 (m), 479 (w, δNCS).

3.2.4. *trans-[Fe(BPM)$_2$(NCS)$_2$] (**9**) crystal structure data*

Crystal data together with refinement details are presented in Table 1. A colourless plate like crystal was attached to a thin glass fibre and mounted on a Rigaku AFC7R diffractometer employing graphite monochromated Cu–K$_\alpha$ radiation generated from a rotating anode. Cell constants were obtained from a least-squares refinement against 25 reflections located between 77 and 103° 2θ. Data were collected at 295(2) K with $\omega-2\theta$ scans to a maximum 2θ value of 120.12°. Processing and subsequent calculations were undertaken with TEXSAN [34]. The intensities of three standard reflections measured every 150 reflections changed by 3.61% during the data collection and a correction was accordingly applied to the data. Lorentz and polarisation corrections were applied to the data, as was an empirical absorption correction based on azimuthal scans of three reflections [35]. The structure was solved in the space group $P2_1/a$ (#14) by direct methods with SIR92 [31], and extended and refined with SHELXL97 [32] using the TEXSAN interface. Anisotropic displacement parameters were refined for the non-hydrogen of the structure model and a riding atom model was used for the model hydrogen atoms. The metal resides on an inversion centre, such that the full complex is generated with $1-x$, $-y$, $-z$. An ORTEP [33] depiction of the molecule with 20% displacement ellipsoids is provided in Fig. 2.

3.2.5. *Synthesis of [Fe(BPM)$_2$Cl]$^+$(BPh$_4$)$^-$ (**7**)*

A solution of [FeCl$_2$] (23 mg, 0.182 mmol) in hot ethanol (5 ml) was added drop-wise to a stirred solution of BPM (**3**) (54.3 mg, 0.367 mmol) in hot ethanol (5 ml). The resultant clear yellow solution was refluxed as a solution of NaBPh$_4$ (700 mg, 2.05 mmol) in hot ethanol (5 ml) was slowly added. As the NaBPh$_4$ was added, a white precipitate began to form. The solution was refluxed for 5 min, then allowed to stand undisturbed overnight. The precipitate was collected by filtration, washed with ethanol (2 × 1 ml) and hexane (2 × 2 ml), and dried in vacuo to give [Fe(BPM)$_2$Cl]$^+$(BPh$_4$)$^-$ (**7**) as a white powder (110 mg, 85%).

M.p. decomposes at 230 °C, melts at 261–262 °C. ^{1}H-NMR (400 MHz, d^4-methanol, 233 K): δ 8.14 (bs, 4H, **H**3 or **H**5(BPM)), 7.77 (bs, 4H, **H**3 or **H**5(BPM)), 7.29 (bs, 8H, *ortho*-**BPh**$_4$), 7.02 (bs, 8H, *meta*-**BPh**$_4$), 6.89 (bs, 4H, *para*-**BPh**$_4$), 6.60 (bs, 4H, **H**4 or **H**1′(BPM)), 6.56 (s, 4H, **H**4 or **H**1′(BPM)) ppm. ^{13}C{^{1}H}-NMR (100 MHz, d^4-MeOH, 240 K): δ 165.3 (q, $^1J_{BC} = 49.1$ Hz, *ipso*-**BPh**$_4$), 142.2 (**C**3), 137.5 (*ortho*-**BPh**$_4$), 132.4 (**C**5), 126.6 (*meta*-**BPh**$_4$), 123.0 (*para*-**BPh**$_4$), 108.1 (**C**4), 65.5 (**C**1′) ppm. (Found: **C**, 64.3; **H**, 4.9; **N**, 15.7. $C_{38}H_{36}N_8BClFe$ requires **C**, 64.57; **H**, 5.13; **N**, 15.85%.) IR ν_{max} cm^{-1} (polyethylene, diffuse reflectance): 408 (s, Fe–Cl), 277 (s, Fe–N(BPM)). Mass spectrum (ESI–methanol) m/z: 449 (24, M$^+$+24, $C_{14}H_{16}N_8ClFe$+NaH, [Fe(BPM)$_2$Cl]$^+$+1H+1Na), 411 (100, M$^+$, $C_{14}H_{16}N_8ClFe$, [Fe(BPM)$_2$Cl]$^+$), 323 (29), 295 (64), 263(46).

3.3. *Synthesis of bis(3,5-dimethyl-1-pyrazolyl)methane (dmBPM) iron(II) complexes*

3.3.1. *Synthesis of [Fe(dmBPM)$_2$Cl$_2$] (**6**)*

[Fe(dmBPM)$_2$Cl$_2$] (**6**) was synthesised using a modified method of Mani [13]. A solution of [FeCl$_2$] (21 mg, 0.166 mmol) in warm ethanol (2 ml) was added drop-wise to a stirred solution of dmBPM (**4**) (54 mg, 0.265 mmol) in warm ethanol (3 ml). The clear yellow solution was heated and stirred for 10 min and a precipitate began to form. The reaction mixture was allowed to stand undisturbed overnight. The precipitate was collected by filtration, washed with ethanol (2 × 1 ml) and hexane (2 × 2 ml), and dried in vacuo to give [Fe(dmBPM)$_2$Cl$_2$] (**6**) as a white powder (49.7 mg, 56%).

M.p. decomposes at 230 °C, melts at 240–241 °C. ^{1}H-NMR (400 MHz, d^4-methanol, 228 K): δ 6.30 (bs, 4H, **H**4 or **H**1′), 6.11 (bs, 4H, **H**4 or **H**1′), 2.64 (bs, 12H, C3-C**H**$_3$ or C5-C**H**$_3$), 2.36 (bs, 12H, C3-C**H**$_3$ or C5-C**H**$_3$). IR ν_{max} cm^{-1} (polyethylene, diffuse reflectance) 350 (s, *cis*-Fe–Cl), 322 (m, *cis*-Fe–Cl), 278 (s, Fe–N(BPM)) ppm. Mass spectrum (CI, CH$_4$, *m*/*z* (%)): 535 (4, M$^+$ + 1, $C_{22}H_{32}N_8Cl_2Fe$ + 1H, [Fe(dmBPM)$_2$Cl$_2$] + 1H), 499 (100, M$^+$ − 1Cl, $C_{22}H_{32}N_8C_2Fe$, [Fe(dmBPM)$_2$Cl]$^+$), 439 (12), 21 (5), 407(48).

3.3.2. *Synthesis of [Fe(dmBPM)$_2$Cl]$^+$(BPh$_4$)$^-$ (**8**)*

[Fe(dmBPM)$_2$Cl]$^+$(BPh$_4$)$^-$ (**8**) was synthesised using a modified method of Mani [13].

A solution of [FeCl$_2$] (20 mg, 0.158 mmol) in hot ethanol (5 ml) was added drop-wise to a stirred solution of dmBPM (**4**) (61.2 mg, 0.299 mmol) in hot ethanol (5 ml). The clear yellow solution was refluxed as a solution of NaBPh$_4$ (60 mg, 0.175 mmol) in hot ethanol (5 ml) was added slowly. As the NaBPh$_4$ was added, the solution became white and cloudy. The solution was refluxed for 5 min, then allowed to stand undisturbed overnight. The precipitate was collected by filtration, washed with ethanol (2 × 1 ml) and hexane (2 × 2 ml), and dried in vacuo to give [Fe(dmBPM)$_2$Cl]$^+$(BPh$_4$)$^-$ (**8**) as a white powder (84 mg, 75%).

M.p. decomposes at 180 °C, melts at 222–230 °C. ^{1}H-NMR (400 MHz, d^4-methanol, 228 K): δ 7.36 (bs, 8H, *ortho*-B**Ph**$_4$), 7.11 (bs, 8H, *meta*-B**Ph**$_4$), 6.99 (bs, 4H, *para*-B**Ph**$_4$), 6.22 (bs, 4H, **H**4 or **H**1′), 6.11 (bs, 4H, **H**4 or **H**1′), 2.62 (s, 12H, C3-C**H**$_3$ or C5-C**H**$_3$), 2.36 (s, 12H, C3-C**H**$_3$ or C5-C**H**$_3$) ppm. ^{13}C{^{1}H}-NMR (100 MHz, d^4-MeOH, 230K): δ 165.4 (q, $^1J_{BC}$ = 49.1 Hz, *ipso*-B**Ph**$_4$), 150.2 (**C**3 or **C**5), 142.9 (**C**3 or **C**5), 137.5 (*ortho*-B**Ph**$_4$), 126.7 (*meta*-B**Ph**$_4$), 123.0 (*para*-B**Ph**$_4$), 107.6 (**C**4), 60.4 (**C**1′), 13.6 (C3-**C**H$_3$ or C5-**C**H$_3$), 11.6 (C3-**C**H$_3$ or C5-**C**H$_3$) ppm. IR ν_{max} cm^{-1} (polyethylene, diffuse reflectance) 352 (br, Fe–Cl), 278 (s, Fe–N(dmBPM)). Mass spectrum (CI, CH$_4$, *m*/*z* (%)): 499 (4, M$^+$, $C_{22}H_{32}N_8ClFe$, [Fe(dmBPM)$_2$Cl]$^+$), 407 (18), 369 (100), 353 (5), 341 (12), 330 (17), 313 (71).

3.4. *Synthesis of tris(1-pyrazolyl)methane (TPM) iron(II) complexes*

3.4.1. *Synthesis of [Fe(TPM)$_2$]$^{2+}$(Cl$^-$)$_2$ (**10**)*

[Fe(TPM)$_2$]$^{2+}$(Cl$^-$)$_2$ (**10**) was synthesised using a modification of the method of Mani [13].

A yellow solution of [FeCl$_2$] (45.6 mg, 0.360 mmol) in warm ethanol (2 ml) was added drop-wise to a stirred solution of TPM (**2**) (155 mg, 0.724 mmol) in warm ethanol (3 ml) resulting in a light purple solution. The reaction mixture was heated and stirred for 10 min, then allowed to stand undisturbed overnight during which time a precipitate formed. The precipitate was collected by filtration and recrystallised from an ethanol and acetone mixture and dried under reduced pressure to give the product, [Fe(TPM)$_2$]$^{2+}$(Cl$^-$)$_2$ (**10**), as pale purple crystals (150 mg, 75%).

M.p. decomposes at 152 °C, melts at 319–320 °C. ^{1}H-NMR (400 MHz, d^4-methanol, 228 K): δ 10.21 (s, 2H, **H**1′), 8.94 (s, 6H, **H**3 or **H**5(TPM)), 7.67 (s, 6H, **H**3 or **H**5(TPM)), 6.90 (s, 6H, **H**4(TPM)) ppm. Mass spectrum (CI, NH$_3$, *m*/*z* (%)): 260 {100, ((M^{2+})/2) + 18, [$C_{20}H_{20}N_{12}Cl_2Fe$]$^{2+}$ + 1H + NH$_3$, [Fe(TPM)$_2$]$^{2+}$ 1H + NH$_3$}.

IR ν_{max} cm^{-1} (KBr powder, diffuse reflectance): 1410 (s), 1280 (s), 1251 (m), 1093 (s), 1060 (m), 785 (vs), 760 (s), 732 (vs), 706 (vs), 613 (m).

3.4.2. *Synthesis of [Fe(TPM)(NCS)$_2$] (**11**)*

A magenta solution of [Fe(NCS)$_2$] (30.1 mg, 0.175 mmol) in warm methanol was added to a solution of TPM (**1**) (40 mg, 0.187 mmol) in warm methanol (5 ml). Upon addition of the [Fe(NCS)$_2$] solution, the reaction mixture changed colour from magenta, to bright yellow, to orange, then finally to red. The reaction mixture was allowed to stand for 3 h then the solvent was removed under reduced pressure and the residue was washed with hexane (3 × 2 ml) to remove excess ligand. The product, [Fe(TPM)(NCS)$_2$] (**11**), was obtained as a light purple solid (24 mg, 35%).

^{1}H-NMR (400 MHz, d^4-MeOH, 250 K): δ 8.90 (s, 1H, **H**1′), 7.94 (s, 3H, **H**3 or **H**5(TPM)), 7.85 (s, 3H, **H**3 or **H**5(TPM)), 6.61 (s, 3H, **H**4(TPM)) ppm. IR ν_{max} cm^{-1} (KBr powder, diffuse reflectance): 3141 (w), 3115 (w), 3102 (w), 382 (w), 2058 (vs, CN(NCS)), 1653 (m), 1559 (s), 1540 (m), 1507 (s), 1456 (s), 1412 (m), 1291 (m), 1089 (m), 1058 (m), 868 (m), 790 (m), 764 (m), 751 (m), 606 (w, δNCS). Mass spectrum (CI, NH$_3$, *m*/*z* (%)): 389 {12, M$^+$ + 3, $C_{12}H_{10}N_8S_2Fe$ + 3H, [Fe(TPM)(NCS)$_2$] + 3H}, 388 {42, M$^+$ + 2, $C_{12}H_{10}N_8S_2Fe$ + 2H, [Fe(TPM)(NCS)$_2$] + 2H}, 382 (22), 371 (20), 346 (95, M$^+$ − 1NCS + 4H + 1NH$_3$, $C_{12}H_{10}N_7S_2Fe$ + 4H + 1NH$_3$, [Fe(TPM)(NCS)] + 4H + 1NH$_3$), 344 (100, M$^+$ −

1NCS+2H+1NH$_3$, $C_{12}H_{10}N_7Sfe$+2H+1NH$_3$, [Fe(TPM)(NCS)]+2H+1NH$_3$), 329 (37%, M^+−1NCS+2H, [$C_{12}H_{10}N_7SFe$]+2H, [Fe(TPM)(NCS)]+2H), 327 (41, M^+−1NCS, $C_{12}H_{10}N_7SFe$, [Fe(TPM)(NCS)]), 308 (33), 300 (17), 291 (67), 279 (27), 263 (43).

4. Conclusions

Three novel iron(II) complexes were synthesised using the bidentate ligand, bis(1-pyrazolyl)methane (BPM, **3**), *cis*-[Fe(BPM)$_2$Cl$_2$] (**5**), *trans*-[Fe(BPM)$_2$(NCS)$_2$] (**9**) and [Fe(BPM)$_2$Cl]$^+$(BPh$_4$)$^-$ (**7**). The X-ray crystal structures of the neutral complexes, (**5**) and (**9**), showed that the two BPM ligands were bound *cis* to one another in the *cis*-[Fe(BPM)$_2$Cl$_2$] (**5**) complex while they were bound mutually *trans* in the complex *trans*-[Fe(BPM)$_2$(NCS)$_2$] (**9**). The ^{1}H-NMR spectra of the complexes, (**5**), (**9**) and (**7**), showed that there was a plane of symmetry through each BPM ligand of each complex. The infrared and far infrared spectra of *cis*-[Fe(BPM)$_2$Cl$_2$] (**5**) and *trans*-[Fe(BPM)$_2$(NCS)$_2$] (**9**) confirmed the relative coordination of the two BPM ligands in both complexes, and also confirmed that the NCS ligands of *trans*-[Fe(BPM)$_2$(NCS)$_2$] (**9**) behaved as isothiocyanato ligands, binding to the iron centre through their N atoms.

Two iron(II) complexes containing the bis(3,5-dimethyl-1-pyrazolyl)methane (dmBPM, **4**) ligand were also synthesised [Fe(dmBPM)$_2$Cl$_2$] (**6**) and [Fe(dmBPM)$_2$Cl]$^+$(BPh$_4$)$^-$ (**8**). As was observed for the iron(II) BPM complexes, the ^{1}H-NMR spectra of each of the complexes, (**6**) and (**8**), showed that there was a plane of symmetry through each dmBPM ligand. The infrared and far infrared spectra of [Fe(dmBPM)$_2$Cl$_2$] (**6**) showed the relative coordination of the two chloro ligands was *cis*.

The *tris*(1-pyrazolyl)methane (TPM, **1**) ligand was used in the synthesis of [Fe(TPM)$_2$]$^{2+}$(Cl$^-$)$_2$ (**10**) which is an analogue of [Fe(TPM)$_2$]$^{2+}$(Br$^-$)$_2$ [13], and [Fe(TPM)(NCS)$_2$] (**11**). The ^{1}H-NMR spectra of each of the complexes, (**10**) and (**11**), showed that the complexes were symmetrical. The newly synthesised complex of iron with TPM, [Fe(TPM)(NCS)$_2$] (**11**) is monomeric, unlike the previously reported polymeric complex [Fe(TPM)(NCS)$_2$]$_n$ [13].

5. Supplementary material

The crystal structure data has been deposited at the Cambridge Crystallographic Data Centre and allocated the deposition numbers CCDC 167929 (complex **5**) and CCDC 167930 (complex **9**). Copies of this information may be obtained free of charge from The Director, CCDC, 12 Union Road, Cambridge CB2 1EZ, UK (Fax: +44-1223-336033; e-mail: deposit@ccdc.cam.ac.uk or www: http://www.ccdc.cam.ac.uk).

Acknowledgements

We gratefully acknowledge financial support from the Australian Research Council (ARC) and the University of Sydney for H.B. and F.M. Gritton Scholarship (L.P.S.).

References

[1] H. tom Dieck, R. Diercks, Angew. Chem. Int. Ed. Engl. 22 (1983) 778.
[2] H. tom Dieck, J. Dietrich, Angew. Chem. Int. Ed. Engl. 24 (1985) 781.
[3] See for example: (a) A. Cotton, G. Wilkinson, C.A. Murillo, M. Bochmann, in: Advanced Inorganic Chemistry, Wiley, 1999, pp. 796–814;
(b) D.H. Flint, R.M. Allen, Chem. Rev. 96 (1996) 2315;
(c) B.J. Waller, J.D. Lipscomb, Chem. Rev. 96 (1996) 2625.
[4] (a) S. Trofimenko, in: S.J. Lippard (Ed.), The Coordination Chemistry of Pyrazole-Derived Ligands, vol. 34, Wiley, New York, 1986;
(b) S. Trofimenko, Chem. Rev. 93 (1993) 943.
[5] (a) S.J. Lippard, W.H. Armstrong, J. Am. Chem. Soc. 107 (1985) 3730;
(b) S.J. Lippard, P.N. Turowski, W.H. Armstrong, M.E. Roth, J. Am. Chem. Soc. 112 (1990) 681;
(c) R.S. Czernuszewicz, J.E. Sheats, T.G. Spiro, Inorg. Chem. 26 (1987) 2063.
[6] N. Kitajima, H. Fukui, Y.J. Moro-oka, J. Chem. Soc. Chem. Commun. (1988) 485.
[7] (a) S. Trofimenko, J. Am. Chem. Soc. 89 (1967) 3170;
(b) S. Trofimenko, J. Am. Chem. Soc. 89 (1967) 6288.
[8] (a) Y. Sohrin, H. Kokusen, M. Matsui, Inorg. Chem. 34 (1995) 3928;
(b) T. Buchen, P. Gutlich, Inorg. Chim. Acta 231 (1995) 221;
(c) J.K. Beattie, R.A. Binstead, R.J. West, J. Am. Chem. Soc. 100 (1978) 3044;
(d) J.P. Jesson, J.F. Weiher, J. Chem. Phys. 46 (1967) 1995.
[9] R.B. King, A. Bond, J. Am. Chem. Soc. 96 (1974) 1334.
[10] W.B. Tolman, D.D. LeCloux, M.C. Keyes, M. Osawa, V. Reynolds, Inorg. Chem. 33 (1994) 6361.
[11] S. Trofimenko, J. Am. Chem. Soc. 92 (1970) 5118.
[12] J.J. McGarvey, H. Toftlund, A.H.R. Al-Obaidi, K.P. Taylor, S.J. Bell, Inorg. Chem. 32 (1993) 2469.
[13] F. Mani, Inorg. Nucl. Chem. Lett. 15 (1979) 297.
[14] A. Macchioni, G. Bellachioma, G. Cardaci, V. Gramlich, H. Ruegger, S. Terenzi, L.M. Venanzi, Organometallics 16 (1997) 2139.
[15] P.A. Anderson, T. Astley, M.A. Hitchman, F.R. Keene, B. Moubaraki, K.S. Murray, B.W. Skelton, E.R.T. Tiekink, H. Toftlund, A.J. White, J. Chem. Soc. Dalton (2000) 3505.
[16] (a) D.L. Reger, C.A. Little, V.G. Young, Jr., M. Pink, Inorg. Chem. 40 (2001) 2870;
(b) D.L. Reger, C.A. Little, A.L. Rheingold, M. Lam, L.M. Liable-Sands, B. Rhagitan, T. Concolino, A. Mohan, G.J. Long, V. Briois, F. Grandjean, Inorg. Chem. 40 (2001) 1508.
[17] (a) A.F. Hill, J.M. Malget, J. Chem. Soc. Dalton Trans (1997) 2003;

(b) A. Pizzano, L. Sanchez, E. Gutierrez, A. Monge, E. Carmona, Organometallics 14 (1995) 14;

(c) I.B. Gorrell, A. Looney, G. Parkin, A.L. Rheingold, J. Am. Chem. Soc. 112 (1990) 4068;

(d) A.F. Hill, G.R. Owen, A.J.P. White, D.J. Williams, Angew. Chem. Int. Ed. 38 (1999) 2759;

(e) J.S. Yeston, R.G. Bergman, Organometallics 19 (2000) 2947.

[18] B.M. Foxman, E.H. Witten, W.M. Reiff, K. Lazar, B.W. Sullivan, Inorg. Chem. 24 (1985) 4585.

[19] I.G. Dance, A.S. Abushamleh, H.A. Goodwin, Inorg. Chim. Acta 43 (1980) 217.

[20] B.N. Figgis, J.M. Patrick, P.A. Reynolds, B.W. Skelton, A.H. White, P.C. Healy, Aust. J. Chem. 36 (1983) 2043.

[21] E. Konig, K.J. Watson, Chem. Phys. Lett. 6 (1970) 457.

[22] M. Konno, M. Mikami-Kido, Bull. Chem. Soc. Jpn. 64 (1991) 339.

[23] K. Nakamoto, P.J. McCarthy, Spectroscopy and Structure of Metal Chelate Compounds, Wiley, New York, 1968.

[24] K. Nakamoto, Infrared and Raman Spectra of Inorganic and Coordination Compounds, 4th ed., Wiley, New York, 1986.

[25] R.H. Crabtree, The Organometallic Chemistry of Transition Metals, 2nd ed., Wiley, New York, 1994.

[26] B.L. Ackerman, J.E. Coutant, Matrix section in the analysis of peptides using fast atom bombardment mass spectrometry, unpublished results, Merrell Dow Research Institute, 1988.

[27] G.J. Leigh, D.L. Hughes, M. Jimenez-Tenorio, A.T. Rowley, J. Chem. Soc. Dalton Trans. (1993) 75.

[28] L.J. Farrugia, J. Appl. Crystallogr. 32 (1999) 837.

[29] J. De Meulenaer, H. Tompa, Acta Crystallogr. 19 (1965) 1014.

[30] TEXSAN for Windows: Single Crystal Structure Analysis Software, Molecular Structure Corporation (1997–1998), MSC, 3200 Research Forest Drive, The Woodlands, TX 77381, USA.

[31] A. Altomare, M. Cascarano, C. Giacovazzo, A.J. Guagliardi, Appl. Crystallogr. 26 (1993) 343.

[32] G.M. Sheldrick, SHELXL97. Program for crystal structure refinement, University of Göttingen, Germany, 1997.

[33] (a) C.K. Johnson, ORTEPII. Report ORNL-5138, Oak Ridge National Laboratory, Oak Ridge, TN, 1976;

(b) S.R. Hall, D.J. du Boulay, R. Olthof-Hazekamp (Eds.), XTAL3.6 System, University of Western Australia, 1999.

[34] TEXSAN: Crystal Structure Analysis Package, Molecular Structure Corporation, 1985 and 1992.

[35] A.C.T. North, D.C. Phillips, F.S. Mathews, Acta Crystallogr. Sect. A 23 (1968) 351.